

Measurements of Modulated Lamellar $P_{\beta'}$ Phases of Interacting Lipid Membranes

Daniel C. Wack^(a) and Watt W. Webb

School of Applied and Engineering Physics, Cornell University, Ithaca, New York 14853-2501

(Received 13 June 1988)

A diffraction study of lattice constants in the $P_{\beta'}$ ("rippled") phase of hydrated lecithins suggests that the lamellar modulation arises from a delicate interplay between the energies associated with membrane curvature and with hydration, as modified by interactions between membranes. Our results imply the existence of a Lifshitz point in the global phase diagram of the lecithin-water system.

PACS numbers: 64.70.Md, 61.30.Eb, 87.15.-v

We report here the results of a systematic high-resolution x-ray diffraction study of the modulated ("rippled," or $P_{\beta'}$) membrane phase of hydrated multilamellar diacylphosphatidylcholines (lecithin).¹ Our data for the dependence of the mean membrane thickness \bar{d}_l and ripple wave vector Q_r on the hydrocarbon chain length N_c and the degree of hydration combine with existing thermodynamic data to yield a simple physical mechanism for modulated-membrane-phase stability. The data support a phenomenological model of structural phase transitions in interacting membranes recently proposed by Goldstein and Leibler.² Hydration interactions, which are supposed to dominate only at small intermembrane spacings,^{3,4} play a central role throughout the $P_{\beta'}$ phase. The systematic trends imply the existence of a Lifshitz multicritical point⁵ within the global lecithin phase diagram, which appears to be accessible by variation of N_c and water composition.

Figure 1 displays the schematic phase boundaries of lecithin in the vicinity of the $P_{\beta'}$ phase. At full hydration the $P_{\beta'}$ phase appears intermediate to the high-temperature, fluid phase L_a and the low-temperature, solidlike phase $L_{\beta'}$. Latent heats ΔH_m at the upper or "main" transition T_m are proportional to chain length N_c , while those at the lower or "pretransition" T_p are independent of N_c .^{6,7} This trend suggests that the pretransition is dominated by membrane surface energetics. As the water content is decreased, the phase terminates at a third triple point T_3 , which is found at water volume fraction $\phi_w \approx 0.18$.⁸ Previous x-ray diffraction studies^{1,9} of the $P_{\beta'}$ phase have indicated that membrane stacking and rippling periodicities show the symmetry of a 2D monoclinic lattice, with constants insensitive to temperature but strongly dependent on ϕ_w . In this study we measured diffraction patterns of structures found along isothermal paths through the single-phase region, as indicated by the dashed line in Fig. 1. We varied hydrocarbon chain lengths over the range $N_c = 12$ to 19, to obtain a set of structural measurements in states of comparable hydration interaction.

Powder diffraction samples were prepared by our mixing weighed amounts of distilled water and synthetic lecithin and inserting them in a 1.0-mm quartz x-ray capil-

lary, which was then sealed. Measured weight fractions of water c_w and lipid c_l were converted to volume fraction of water by $\phi_w = c_w v_w / (c_w v_w + c_l v_l)$, where we assume that the partial specific volume of water v_w is equivalent to the bulk value, and we take the partial specific volume of lipid v_l for each N_c in the $P_{\beta'}$ phase from the measurements of Nagle and Wilkinson.⁶ The capillaries were equilibrated in an evacuated cell whose temperature was controlled to $\pm 0.1^\circ\text{C}$ by thermoelectric elements. High-resolution synchrotron x-ray diffraction experiments were performed on the A3 line at the Cornell High Energy Synchrotron Source with a horizontally focused 8.3-keV beam. With film recording, the width of the experimental resolution function was $\approx 7 \times 10^{-4} \text{ \AA}^{-1}$, and with a linear position-sensitive detector, it was $\approx 2 \times 10^{-3} \text{ \AA}^{-1}$. Lattice constants were

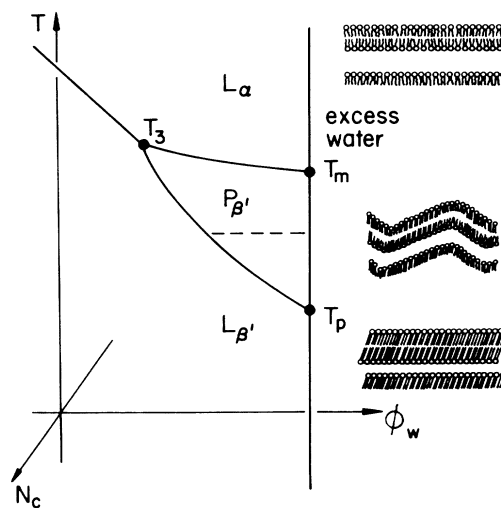


FIG. 1. Schematic lecithin-water phase diagram near full hydration. The triple point T_3 ($P_{\beta'} \leftrightarrow L_a + L_{\beta'}$) occurs at $\phi_w \approx 0.18 \pm 0.01$. Dashed line represents the isothermal paths explored in this study, midway between the triple points T_m and T_p . For hydrocarbon chain lengths $N_c = 12$ to 19, these temperatures were $-7.0, 7.0, 18.0, 28.0, 39.0, 45.5, 53.0,$ and 59.1°C , respectively. Drawings at right suggest the physical state of the phospholipid bilayer in each fully hydrated phase.

derived by a nonlinear least-squares fit of a 2D monoclinic formula to the observed positions. A full description of the experimental details and additional results will be published elsewhere.¹⁰

All P_β samples showed a "low-angle" ($|Q| < 0.6 \text{ \AA}^{-1}$) powder pattern which could be indexed on a 2D monoclinic lattice with constants d_s , λ_r , and θ_m being the stacking distance, ripple wavelength, and monoclinic angle, respectively. For $\phi_w \lesssim 0.30$, powder samples showed 20 to 25 resolution-limited peaks, but at higher water contents increased disorder both weakened higher-order peaks and smeared closely spaced one. Lattice-constant data are shown only for those samples having at least six resolved and unambiguously indexed peaks. When the position of the ripple wave vector $Q_r(l) \equiv 2\pi l/\lambda_r$ did not overlap other peaks, harmonics $l=2$ to 4 were visible, and showed structure factors greater in magnitude than the fundamental. The structural implications of this feature will be discussed elsewhere.¹⁰ For all N_c , θ_m was $\approx 98^\circ$ for $\phi_w \lesssim 0.25$ but decreased towards 90° as ϕ_w increased. To represent the total repeat spacing normal to the average layer position, we form the quantity $d_t = d_s \sin\theta_m$. By use of the calculated volume fraction ϕ_w , this total spacing can be decomposed into mean lipid and mean water layer thicknesses, \bar{d}_l and \bar{d}_w . Finally, using the volume per lipid molecule V_l , we can obtain the mean projected area per head group at the aqueous interface: $\bar{A}_l = 2V_l/\bar{d}_l$. We found that \bar{d}_w increased linearly with ϕ_w for all N_c up to the highest water contents explored ($\phi_w \approx 0.38$). We present the structural analysis as a function of the water thickness \bar{d}_w to compare states of equal hydration interaction strength.

Figure 2 summarizes our measurements of the structural properties of modulated lecithin membranes. The first two panels show that, for all N_c , the mean membrane thickness \bar{d}_l increases as the separation decreases, with the area per head group \bar{A}_l following inversely. At a fixed membrane separation, while \bar{A}_l is independent of N_c , \bar{d}_l increases with N_c at the rate of 0.20 nm per CH_2 pair. The cross section normal to the chain axis of a pair of hydrocarbon chains packed in a hexagonal array is $\approx 0.40 \text{ nm}^2$, and the increment along the chain axis per CH_2 pair is $\approx 0.25 \text{ nm}$. The regular increase of \bar{d}_l at fixed \bar{A}_l implies that chain conformation and molecular tilt are constant. The values of \bar{d}_l and \bar{A}_l imply extended chains tilted at $\approx 37^\circ$ with respect to the mean membrane normal.

Figure 2(c) displays the modulation wave vector $Q_r \equiv 2\pi/\lambda_r$. We find that near full hydration, Q_r decreases slowly with \bar{d}_w , but it also scales inversely with N_c , and thus inversely with the membrane thickness \bar{d}_l . To identify the effects of membrane hydration, we eliminate the variations with \bar{d}_l by defining a reduced modulation wave vector $\bar{Q}_r \equiv 2\pi\bar{d}_l/\lambda_r$. The values of \bar{Q}_r for each N_c plotted in Fig. 2(d) with use of the data of Figs. 2(a) and 2(c) can almost be reduced to a single curve, within

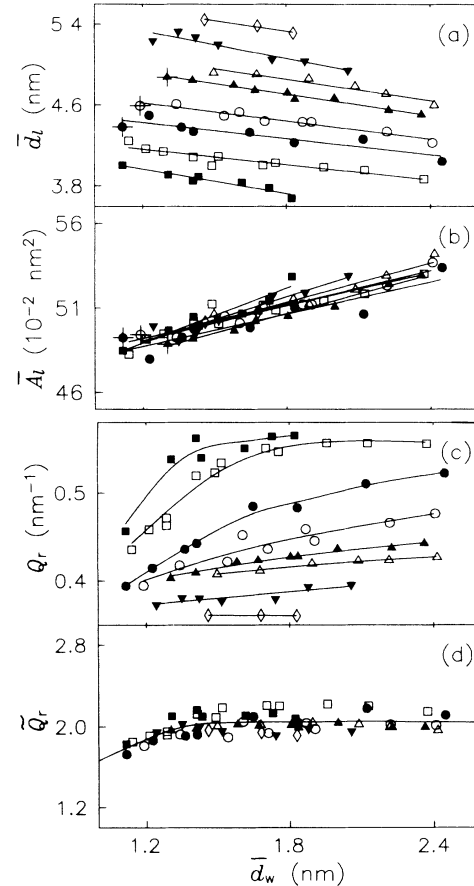


FIG. 2. P_β -phase structural data for $N_c = 12$ to 19, shown sequentially from the lowest to highest curve in (a), plotted as a function of water thickness \bar{d}_w at fixed temperature. (a) Average bilayer thickness \bar{d}_l ; linear fit superimposed. (b) Average projected area per lipid molecule \bar{A}_l . (c) Modulation wavelength λ_r ($\equiv 2\pi/Q_r$), fitted by smoothing splines. (d) Reduced modulation wave vector \bar{Q}_r , with smoothing curve.

the overall accuracy. The limiting values of $\bar{Q}_r \equiv \bar{Q}_0$ at large \bar{d}_w presumably represent the effects of hydration of individual membranes, while the slopes at small \bar{d}_w reveal intermembrane hydration interactions.

By combining our measurements of \bar{d}_l with previous measurements of d_l in the L_α phase,^{4,8,11} we can estimate the fractional change $\Delta\psi_m$ in membrane thickness at T_m near full hydration; i.e., $\Delta\psi_m \equiv [\bar{d}_l(P_\beta) - d_l(L_\alpha)]/d_l(L_\alpha)$. Figure 3 presents $\Delta\psi_m$ as well as the latent heats ΔH_m at T_m . As a function of N_c , both properties extrapolate to zero at roughly $N_c^* = 9-10$, similar to an approach to a critical point. At the simplest level, this can be attributed to the pinning of chain ends to head groups, which prevents a portion $\sim N_c^*$ of the hydrocarbon chain from participating fully in the bulk hydrocarbon-chain melting transition.¹² Thus, by variation of chain length, the melting transition in membranes can be tuned between the quasi-2D regime $N_c \lesssim N_c^*$, in which melting is dom-

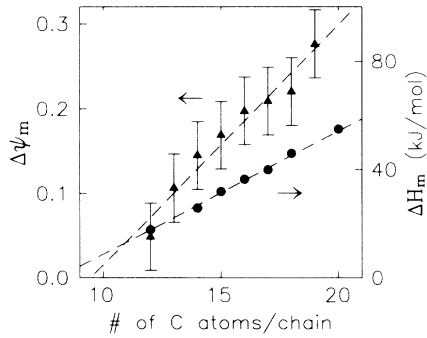


FIG. 3. Fractional change in membrane thickness $\Delta\psi_m$ and latent heats ΔH_m at T_m . Data for $d_l(L_a)$ from Ref. 11, and for ΔH_m from Ref. 7.

inated by translational disordering, and the 3D limit $N_c \gtrsim N_c^*$, dominated by chain conformational disorder.

Goldstein and Leibler have recently proposed a phenomenological model for the lamellar phases of interacting lipid membranes.² It is a continuum theory based on a scalar order parameter ψ proportional to the membrane thickness: $\psi \equiv [d_l(T) - d_0]/d_0$, where d_0 is a reference thickness, taken as that of the fluid phase. The model combines a Landau theory of intramembrane melting transitions and a continuum model of molecular forces between membranes, which are dominated by hydration interactions. The Hamiltonian for an isolated membrane has the form

$$H_0[\psi] = \int d^2x \left\{ \frac{1}{2} \Sigma (\nabla\psi)^2 + \frac{1}{2} K (\nabla^2\psi)^2 + \frac{1}{2} a_2 (T - T_0) \psi^2 + \frac{1}{3} a_3 \psi^3 + \frac{1}{4} a_4 \psi^4 \right\}.$$

T_0 is the critical temperature of a uniform system in the absence of a cubic term. For values of the phenomenological coefficients $a_3 \neq 0$ and Σ sufficiently negative, the model exhibits three phases: $L_a[\psi(x) \equiv 0]$ and $L_\beta[\psi(x) = \text{const} > 0]$ which are planar phases, and at intermediate temperatures, a modulated phase $P_\beta[\psi = \psi(x)]$. The model predicts that at the $P_\beta \leftrightarrow L_a$ transition $Q_r \equiv (|\Sigma|/2K)^{1/2} > 0$, except when $\Sigma = a_2 = a_3 = 0$, which corresponds to a Lifshitz point.⁵ At this point the wavelength of the modulation diverges.

The continuum model for molecular interactions between neutral membranes includes contributions of van der Waals attraction and the "hydration" repulsion. Measurements on L_a and L_β membranes^{3,4} show that the hydration interaction $V_h(d_w)$ is roughly exponential in form: $V_h(d_w) = H \exp(-d_w/\lambda_h)$, where the decay length $\lambda_h \approx 0.25$ nm, and H is constant of order 0.1–1.0 J/m². The geometrical relation $d_l/d_w = (1 - \phi_w)/\phi_w$ displays the model's coupling between interactions, which are dependent on ϕ_w , and ψ , which is dependent on d_l . We will not show that this model is consistent with our structural analysis of the P_β phase.

Chain length as a scaling field.—The vanishing of

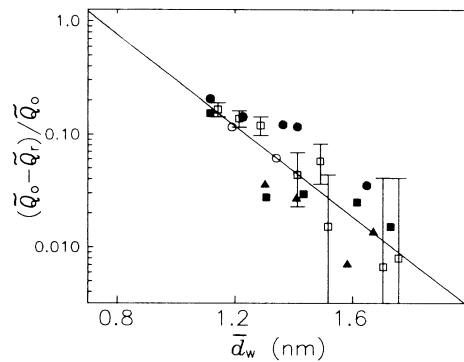


FIG. 4. Fractional change, for $N_c \leq 16$, of reduced modulation wave vector, $(\tilde{Q}_0 - \tilde{Q}_r)/\tilde{Q}_0$, relative to its value at full hydration \tilde{Q}_0 ; solid line is an exponential fit, with slope $\lambda_h = 0.23 \pm 0.03$ nm. Error bars are shown on particularly complete data for $N_c = 13$, and are dominated by the uncertainty in \tilde{Q}_0 (≈ 0.1 nm).

both ΔH_m and $\Delta\psi_m$ at a characteristic value $N_c = N_c^*$ (Fig. 3) is consistent with the appearance of a critical point at $T_m(N_c^*)$ in the scaling field of the parameter N_c which represents the membrane thickness. Extrapolation of known values of $T_m(N_c)$ to N_c^* yields 255 K, which is roughly equal to the critical temperature $T_0 \approx 260$ K indicated by our fitting the model to experimental values of T_m , T_p , and T_3 at fixed N_c . Thus we find that the "mobile" hydrocarbon chain length $N_c - N_c^*$ is an important scaling field in membrane phase behavior.

Coupling of interactions to thickness.—The increase in \bar{d}_l with dehydration [Fig. 2(a)], which parallels behavior observed in L_a and L_β phases,⁴ is consistent with the model's coupling of hydration interactions to the membrane thickness.¹³ Although the order parameter does not distinguish between thickness changes due to tilt and chain conformation, tilt is implicated by our data for \bar{A}_l [Fig. 2(b)].

Membrane curvature energy.—The term $K(\nabla^2\psi)^2$ behaves like membrane curvature energy. Continuum elastic theories for the dependence of membrane rigidity on thickness predict $K \propto (d_l)^y$, $2 \leq y \leq 3$,^{14,15} in which case $Q_r = (|\Sigma|/2K)^{1/2} \propto 1/(\bar{d}_l)^{y/2}$. The scaling of Q_r with membrane thickness [Figs. 2(c) and 2(d)] strongly suggests that membrane curvature energy plays a fundamental role in the modulation energetics.

Coupling of Q_r with \bar{d}_w through intermembrane interactions.—A generalized theory for hydration forces between modulated membranes shows that interactions effectively contribute a positive term to Σ : $\Sigma \rightarrow \Sigma_0 + H_1 \exp(-\bar{d}_w/\lambda_h)$.² Thus the fractional shift of the reduced modulation wave vector from its value \tilde{Q}_0 at full hydration, $(\tilde{Q}_0 - \tilde{Q}_r)/\tilde{Q}_0$, should vary as $\exp(-\bar{d}_w/\lambda_h)$. An exponential fit (Fig. 4) yields a decay length of 0.23 ± 0.03 nm, consistent with the values of λ_h measured in L_a and L_β phases of lecithin.^{3,4} Extrapolation

to $\tilde{Q}_r=0$, where Σ would also vanish, defines a membrane separation $\bar{d}_w^* \approx 0.7 \pm 0.2$ nm, which is equal to the measured membrane separation at the triple point T_3 , within the experimental uncertainty.⁸

Evidence for a Lifshitz point.—The implied accessibility of the state $\Sigma=0$ within the global phase diagram (N_c, T, ϕ_w) for lecithin, together with the scaling of ΔH_m and $\Delta \psi_w$ shown in Fig. 3, suggests that a line of triple points $T_3(N_c, \phi_w)$ ends at a Lifshitz point at $N_c^* \approx 9$ and $\phi_w \approx 0.18$. The systematic variations in Q_r that we observe for $N_c > N_c^*$ can then be attributed to the *proximity* of the Lifshitz point. Structural measurements near the triple point T_3 as a function of N_c (possibly with mixtures of chain lengths to make N_c quasicontinuous) would test the proposal of this multicritical point.

A complete microscopic description of the structural modulation is a difficult problem, whether experimentally or theoretically undertaken, especially if structural defects are significant. The important conclusion of our work is that *many aspects of the global behavior of the P_β phase of lecithin can be understood without reference to the details of the modulated membrane structure.*¹⁰ The systematic structural analysis presented here provides a basis for further microscopic theoretical approaches.

We thank M. B. Schneider and P. E. Cladis for many valuable discussions, R. E. Goldstein and S. Leibler for discussing the details of their theoretical work, and the members of the Cornell High Energy Synchrotron Source staff for their technical assistance. This work

was supported by National Science Foundation Grant No. DMR-8404942, and benefited from the facilities of the Materials Science Center at Cornell University.

-
- ^(a)Present address: GE Co., French Rd., Utica, NY 13503.
- ¹A. Tardieu, V. Luzzati, and F. C. Reman, *J. Mol. Biol.* **75**, 711 (1973).
- ²R. Goldstein and S. Leibler, "Model for Lamellar Phases of Interacting Lipid Membranes" (to be published).
- ³V. A. Parsegian, N. Fuller, and R. P. Rand, *Proc. Natl. Acad. Sci. U.S.A.* **76**, 2750 (1979).
- ⁴L. J. Lis, M. McAlister, N. Fuller, R. P. Rand, and V. A. Parsegian, *Biophys. J.* **37**, 657 (1982).
- ⁵R. M. Hornreich, M. Luban, and S. Shtrikman, *Phys. Rev. Lett.* **35**, 1678 (1975).
- ⁶J. F. Nagle and D. A. Wilkinson, *Biophys. J.* **23**, 159 (1978).
- ⁷G. Cevc and D. Marsh, *Phospholipid Bilayers: Physical Principles and Models* (Wiley, New York, 1987), p. 264.
- ⁸M. J. Janiak, D. M. Small, and G. G. Shipley, *J. Biol. Chem.* **254**, 6068 (1979).
- ⁹Y. Inoko, T. Mitsui, K. Ohki, T. Sekiya, and Y. Nozawa, *Phys. Status Solidi (a)* **61**, 115 (1980).
- ¹⁰D. C. Wack and W. W. Webb, to be published.
- ¹¹B. A. Cornell and F. Separovic, *Biochim. Biophys. Acta* **733**, 189 (1983).
- ¹²A. Seelig and J. Seelig, *Biochem.* **13**, 4839 (1974).
- ¹³See also V. A. Parsegian, *J. Theor. Biol.* **15**, 70 (1967).
- ¹⁴W. Helfrich, in *Physics of Defects*, edited by R. Balian *et al.* (North-Holland, New York, 1981), p. 716.
- ¹⁵A. G. Petrov and I. Bivas, *Prog. Surf. Sci.* **16**, 389 (1984).